Natural gas hydrate formation and decomposition in the presence of kinetic inhibitors. 2. Stirred reactor experiments

Daraboina, Nagu; Linga, Praveen; Ripmeester, John; Walker, Virginia K.; Englezos, Peter

Publisher's version / Version de l'éditeur:
https://doi.org/10.1021/ef200813v
Energy & Fuels, 25, 10, pp. 4384-4391, 2011-08-13

energy&fuels

ARTICLE

pubs.acs.org/EF

Natural Gas Hydrate Formation and Decomposition in the Presence of Kinetic Inhibitors. 2. Stirred Reactor Experiments

Nagu Daraboina,[†] Praveen Linga,[†,‡] John Ripmeester,[§] Virginia K. Walker,[∥] and Peter Englezos*[,†]

[†]Department of Chemical and Biological Engineering, University of British Columbia, Vancouver, British Columbia, Canada

[‡]Department of Chemical and Biomolecular Engineering, National University of Singapore, Singapore

[§]Steacie Institute for Molecular Sciences, National Research Council Canada, Ottawa, Ontario, Canada

[∥]Department of Biology, Queen's University, Kingston, Ontario, Canada

ABSTRACT: A newly fabricated, stirred reactor was used to investigate hydrate inhibition and decomposition in the presence of two commercial, chemical kinetic inhibitors, polyvinylpyrrolidone (PVP) and H1W85281, as well as two antifreeze proteins (AFPs), type I and type III. The longest induction times and the slowest growth rates were observed with HIW8581, with the fastest growth recorded for PVP. Type I AFP (AFP-I) was a more effective inhibitor, with respect to induction time and growth, than either PVP or type III AFP (AFP-III). Complete hydrate decomposition occurred earlier in the presence of any of the inhibitors compared to water controls. However, depending on the type of inhibitor present during crystallization, hydrate decomposition profiles were distinct, with a longer, two-stage decomposition profile in the presence of the chemical kinetic inhibitors (PVP and H1W85281). The fastest, single-stage decompositions were characteristic of hydrates in experiments with either of the AFPs. These results argue that thought must be given to inhibitor-mediated decomposition kinetics in screens and designs of potential kinetic inhibitors. This is a necessary, practical consideration for industry in cases when, because of long shut in periods, hydrate formation may be unavoidable, even when inhibitors are utilized.

I. INTRODUCTION

The unexpected formation of gas hydrates in hydrocarbon production facilities and transportation pipelines can lead to blockages and shutdowns, and therefore, it is a serious economic and safety issue.[1,2] Traditionally, the prevention of hydrate formation has been achieved with the addition of thermodynamic inhibitors, commonly methanol or glycols. However, in the last two decades, economic and environmental factors have motivated research and development to identify alternative low dosage (less than 1 wt %) hydrate inhibitors (LDHIs). Some LDHIs prolong the induction time for hydrate nucleation and reduce growth (kinetic hydrate inhibitors, KHIs) while other LDHIs prevent hydrate crystal agglomeration (antiagglomerants). A large number of synthetic chemicals, mostly polymers, have been explored as potential KHIs.[3,4] Unfortunately, some of these polymers may not readily biodegrade, and therefore, there has been some interest in assessing the utility of biological inhibitors.[4−10]

Antifreeze proteins (AFPs) and antifreeze glycoproteins (AFGPs) are best known from ocean fish that have evolved at high latitudes; these proteins adsorb to embryonic ice crystals and prevent serum freezing in the equilibrium crystallization gap.[11,12] Some of these repetitive proteins derived from polar fish and insects show inhibition activity not only toward ice but also toward tetrahydrofuran (THF), propane, and methane hydrates.[7−9] To our knowledge, only two reports have documented the utility of AFPs to inhibit hydrates formed from a natural gas mixture. Ohno et al[10] used high pressure microdifferential scanning calorimetry (HP-μDSC) with a silica gel medium and reported that biological inhibitors can inhibit natural gas hydrate formation. In addition, Jensen et al.[13] reported that an ice structuring protein was found to outperform polyvinylcaprolactam (PVCap) for both structure I (sI) and structure II (sII) hydrate inhibition. Thus, it is evident that these biological inhibitors can inhibit natural gas hydrate formation, but how well they perform compared to commercial KHIs in an environment that approximates field conditions remains unknown.

The majority of inhibition studies use single hydrate formers rather than gas mixtures because of the inherit complexity of natural gas blends with regard to the different hydrate equilibria, structural characteristics, and diffusion constants of each of the components.[14−16] Even less understood is the decomposition kinetics of mixed gas hydrates in the presence of KHIs. There is evidence that hydrates crystallized in the presence of gas mixtures do not behave like those formed from single gases.[17−20] Nevertheless, understanding hydrate decomposition kinetics and predicting hydrate decomposition rates in the presence of KHIs is important for efficient hydrate plug removal in pipelines.

It is a challenge to model pipeline conditions in the laboratory, but oil and gas companies favor stirred reactors, originally designed by Vysniauskas and Bishnoi,[21] with their utility demonstrated by Bishnoi and his colleagues[22,23] and subsequently modified and used in multiple studies.[9,24,25] Because many biological inhibitors are available in limited quantities, we have fabricated a small scale apparatus (crystallizer volume of 58 cm^3) based on industry-favored reactors. Using this new equipment, we have successfully

Received: June 1, 2011
Revised: August 13, 2011
Published: August 13, 2011

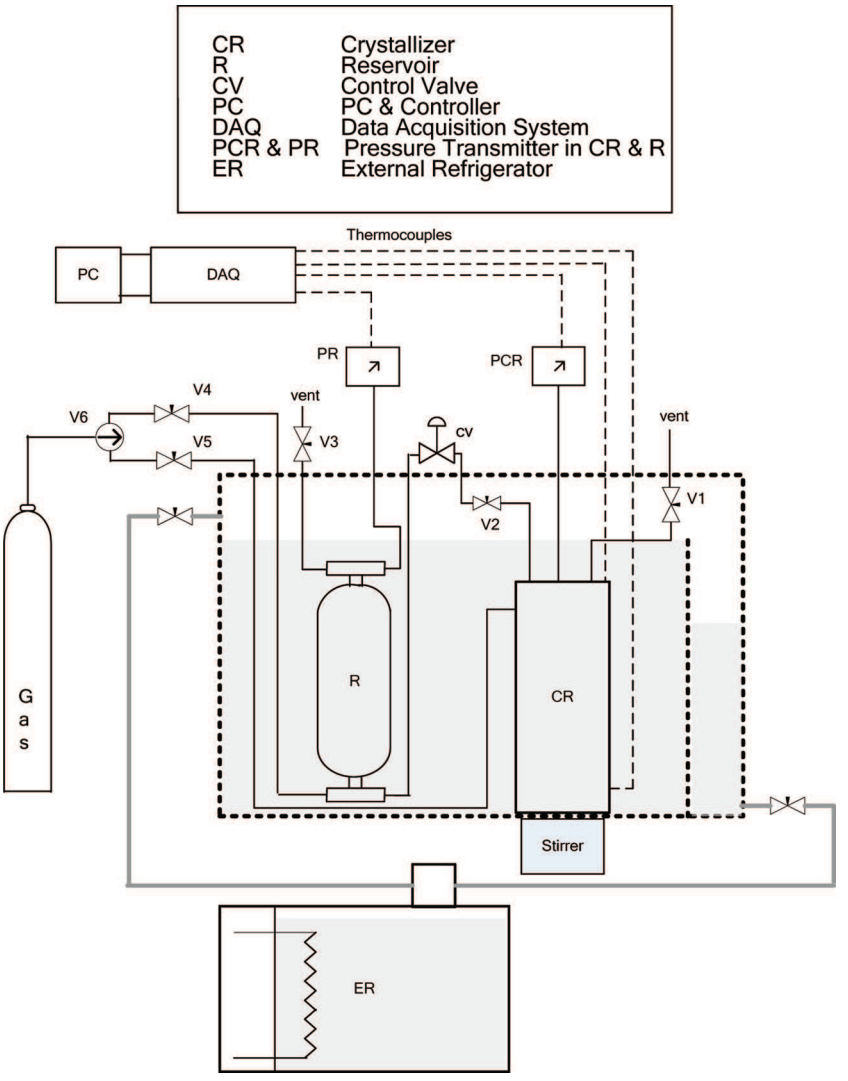

Figure 1. Schematic of the apparatus for hydrate induction and decomposition.

compared two different commercial synthetic inhibitors and two different AFPs for their impact on mixed gas hydrate nucleation, growth, and decomposition.

II. EXPERIMENTAL SECTION

A. Materials. Deionized, distilled water was used to prepare all solutions. Two commercial KHIs were used: polyvinylpyrrolidone (PVP; average molecular weight, ~10 kDa; from Sigma Aldrich) and H1W85281 (average molecular weight, ~3 kDa; a proprietary commercial product of unknown composition). Two fish AFPs purchased from A/F Protein Inc. were used: Type I AFP (AFP-I; average molecular weight, 3.3−4.5 kDa) purified from fish serum and type III AFP (AFP-III; Swiss Prot Database accession number P19414; average molecular weight, 7 kDa), purified after fermentation and secretion from recombinant *Saccharomyces cerevisiae* yeast cells. The methane (93%)/ethane (5%)/propane (2%) gas mixture (UHP grade) was supplied by Praxair Technology Inc.

B. Apparatus. Figure 1 shows a schematic of the apparatus. It consists of a crystallizer (CR) which is a cylindrical vessel (i.d. = 3.00 cm, height = 7.07 cm) made of 316 stainless steel with a volume of 58 cm^3. A 150 cm^3 reservoir (R) supplied gas during hydrate formation in a semibatch operation. The crystallizer and the reservoir were immersed in a temperature-controlled water bath, regulated by an external refrigerator (VWR Scientific). Two Rosemount smart pressure transmitters (model 3051, Norpac controls, Vancouver, BC) with a maximum uncertainty of 0.075% of span 0−15 000 kPa (i.e., 11 kPa) were employed. The temperature of the hydrate phase and the gas phase of the crystallizer was measured using Omega (Omega Engineering, Stamford, CT) copper-constantan thermocouples with an uncertainty of 0.1 K. A valve (Fisher-Baumann) coupled to a PID controller and connected between the reservoir and the crystallizer regulated the flow of gas from the reservoir to the crystallizer and vice versa. The data acquisition system (National Instruments) was coupled with a computer to record the data, as well as to communicate with the control valve, and used LabView 8.0 (National Instruments) software.

C. Hydrate Formation. The hydrate formation procedure is available in detail in the literature.[26] The crystallizer was loaded with KHI solution (10 mL), pressurized with the gas mixture, and then depressurized (at a pressure below the equilibrium hydrate formation pressure) three times in order to remove air from the system. Subsequently, the crystallizer temperature and pressure were set to the desired level, and when this was achieved (approximately 5 min), the stirrer was started. This was set as time zero for the experiments. The aqueous solution in the crystallizer was stirred using a magnetic stirrer at a

Table 1. Experimental Conditions, Induction Times, and Mean Gas Consumption for Methane/Ethane/Propane Gas Hydrate Formation at 275.15 K and 8.1 MPa

gas mixture CH_4 (93%) C_2H_6 (5%) C_3H_8 (2%)	no.	sample state	induction time (min)	moles consumed after 10 h	mean induction time, $\bar{t}_{ind}$ (min)	mean gas consumption, $\bar{n}$ (mol)
water	1	fresh	8.0	0.0167	$\bar{t}_{ind} = 6.2$	$\bar{n} = 0.0173$
	2	memory	4.3	0.0166	$\bar{t}_{ind,fresh} = 7.3$	$\bar{n}_{fresh} = 0.0174$
	3	fresh	6.7	0.0180	$\bar{t}_{ind,memory} = 5$	$\bar{n}_{memory} = 0.0172$
	4	memory	5.7	0.0178		
water + 0.5 wt % PVP	5	fresh	19	0.0157	$\bar{t}_{ind} = 13.5$	$\bar{n} = 0.0151$
	6	memory	12	0.0151	$\bar{t}_{ind,fresh} = 17.3$	$\bar{n}_{fresh} = 0.0153$
	7	fresh	15.7	0.0149	$\bar{t}_{ind,memory} = 9.7$	$\bar{n}_{memory} = 0.0149$
	8	memory	7.4	0.0146		
water + 0.5 wt % HIW85281	9	fresh	292	0.0093	$\bar{t}_{ind} = 208.3$	$\bar{n} = 0.0079$
	10	memory	346	0.0088	$\bar{t}_{ind,fresh} = 182.8$	$\bar{n}_{fresh} = 0.0085$
	11	fresh	73.7	0.0076	$\bar{t}_{ind,memory} = 233.8$	$\bar{n}_{memory} = 0.0081$
	12	memory	121.4	0.0073		
water + 0.5 wt % AFP I	13	fresh	32.0	0.0117	$\bar{t}_{ind} = 19.6$	$\bar{n} = 0.0121$
	14	memory	15.3	0.0109	$\bar{t}_{ind,fresh} = 23.0$	$\bar{n}_{fresh} = 0.0109$
	15	fresh	14.0	0.0101	$\bar{t}_{ind,memory} = 16.2$	$\bar{n}_{memory} = 0.0107$
	16	memory	17.0	0.0104		
water + 0.5 wt % AFP III	17	fresh	8.7	0.0156	$\bar{t}_{ind} = 8.9$	$\bar{n} = 0.0149$
	18	memory	8.0	0.0151	$\bar{t}_{ind,fresh} = 10.2$	$\bar{n}_{fresh} = 0.0152$
	19	fresh	11.7	0.0147	$\bar{t}_{ind,memory} = 7.7$	$\bar{n}_{memory} = 0.0147$
	20	memory	7.3	0.0143		

constant speed (400 rpm). Experiments were routinely conducted at 275.15 K and 8.1 MPa. The equilibrium hydrate formation (structure II) pressure for the gas mixture at 275.15 K is 1.06 MPa.[1] All hydrate formation experiments with and without inhibitors were carried out in a semibatch manner (constant pressure and temperature, with a fixed amount of aqueous solution and continuous supply of gas). The nucleation point or induction time was identified on the basis of a sudden temperature rise or increased gas consumption. Hydrate formation is associated with the incorporation of gas and a consequent drop in crystallizer pressure. Here, constant pressure was maintained with the PID controller. Pressure (P) and temperature (T) measurements were used to calculate the number of moles of gas consumed (gas uptake) by the following equation:[26]

$$\Delta n_H = n_{H,t} - n_{H,0} = \left(\frac{PV}{zRT}\right)_{G,0} - \left(\frac{PV}{zRT}\right)_{G,t} + \left(\frac{PV}{zRT}\right)_{SV,0} - \left(\frac{PV}{zRT}\right)_{SV,t}$$

where n_H is the number of moles consumed to form hydrate (H) or dissolved in water at time t and time 0, z is the compressibility factor calculated by Pitzer's correlation, and V is the volume of the crystallizer.

The memory experiments were conducted using the same procedure explained above except that the memory experiments were started 4 h after the complete decomposition of hydrates formed in fresh solutions.[26]

D. Hydrate Decomposition. After hydrate formation, the crystals were decomposed by heating the water bath from 275 to 295 K at 8.1 MPa at the start of the decomposition experiment, with similar heating profiles for each experiment. Briefly, the procedure is as follows: after the end of the formation experiment, the heater was turned on (time zero for the decomposition experiment) to heat the reactor from 275 to 295 K; the stirrer speed of 400 rpm used for the formation experiment was continued, and the data was recorded for every 20 s. The hydrates start to decompose once the temperature crosses the equilibrium phase boundary, concomitant with an increase in crystallizer pressure. The expansion of gas due to the temperature-mediated increase was calculated by conducting a control experiment with no hydrate formation. The procedure for the control experiment is as follows: water (10 mL) was introduced into the crystallizer, the pressure was set to 8.1 MPa, and the temperature was increased from 275 to 295 K without any mixing. The temperature and pressure were monitored for the control experiments. The difference between the hydrate experiments (gas expansion due to temperature rise and gas released due to hydrate decomposition) and the no-hydrate experiment corresponded to the gas release attributed to hydrate decomposition.

The normalized gas release is calculated as follows:

$$\text{normalized gas release} = n/n_t$$

where n is the number of moles of gas released at any given time in the experiment and n_t is the total number of moles of gas recovered at the end of the experiment.

III. RESULTS AND DISCUSSION

A. Hydrate Nucleation and Growth in the Presence of Inhibitors. As expected, there was a significant delay in the onset of hydrate nucleation, as determined by the longer induction time in the presence of any of the KHIs (Table 1). When all experiments were compared, the commercial inhibitor H1W85281 was the most effective in prolonging the period before nucleation. AFP-I was modestly more effective than PVP and AFP-III (Figure 2). When compared to water controls, hydrate nucleation was delayed by a factor of 1.4 in the presence of AFP-III, 2.2 in the presence of PVP, 3.2 in the presence of AFP-I, and 33.6 in the presence of H1W85281. Overall, average hydrate nucleation times were as follows: water (6.2 min) < AFP-III (8.9 min) < PVP (13.5 min) < AFP-I (19.6 min) < H1W85281 (208.3 min). It is noted that the average hydrate nucleation times in our

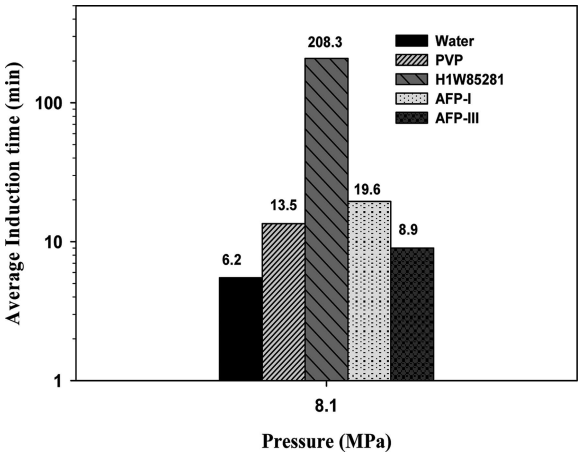

Figure 2. Induction time for hydrate formation in the presence of inhibitors at 8.1 MPa. The scale for the induction time is logarithmic as a result of large differences in the induction times between the inhibitors.

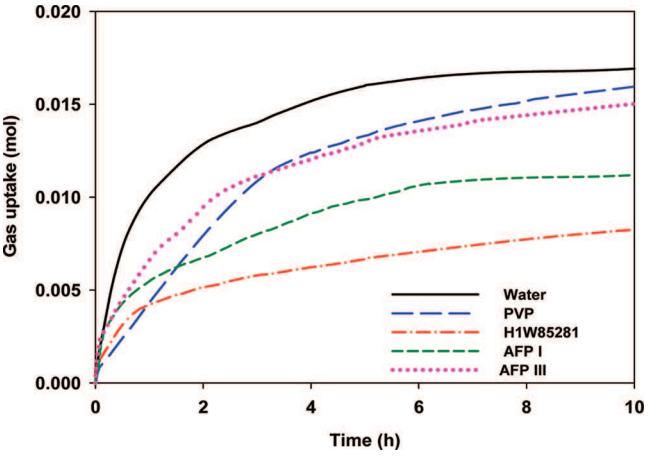

Figure 3. Effect of inhibitors on hydrate growth for experiments conducted at 8.1 MPa and 275.15 K (experiments 1, 5, 9, 13, and 17 from Table 1). Time zero in the graph corresponds to the nucleation point (induction time given in Table 1) for the experiments.

HP-DSC work[27] were in the order water (114 min) < AFP-III (188 min) < PVP (204 min) < H1W85281 (252). The order of the delay of induction in the presence of inhibitors correlates well between HP-DSC (1 μL) and stirred tank reactor (10 mL) results.

The average induction times for recrystallization were always less than with fresh solutions for water controls, PVP, AFP-I, and AFP-III (Table 1). HIW85281 samples did not show this "memory effect".

It is not yet clear what processes govern the hydrate nucleation rate. It has been suggested that KHIs act by adsorbing to heterogeneous nucleators such as impurities in the water phase and the walls of the crystallizer.[6,10] If correct, then H1W85281 is more likely, by an order of magnitude, to interact with such foreign materials, thereby minimizing nucleation sites in order to delay the induction time.

All the inhibitors reduced overall hydrate growth or the moles of gas consumed 10 h after the initial nucleation (Table 1). In the presence of AFP-III and PVP, gas consumption was reduced by 13−14% compared to that seen in water controls. AFP-I reduced gas uptake by 30%, and H1W8528 reduced it by 54%. Thus, the commercial KHI H1W85281 was also the most effective in reducing hydrate growth, concomitant with the superior delay in the onset of hydrate formation.

The impact of the various inhibitors on hydrate formation can be best visualized on a time profile (Figure 3). During the first 5 min, the rate of hydrate growth in the presence of any of the inhibitors was similar to and slower than that of the water controls. Subsequently, the profile changed, and after 120 min, the slowest growth rates were seen with HIW85281 and AFP-I (Figure 3). Hydrate formation in the absence of KHIs reached a plateau in 5−6 h, as expected in a stirred vessel where the nucleation and growth are followed by the state of crystal agglomeration.[28] When inhibitors were present, hydrate formation continued to increase slowly for the duration of the experiment, except for AFP-I, which, similarly to the water samples, appeared to plateau, although at a significantly lower level than the controls.

KHIs are thought to reduce the transport of guest molecules to the hydrate surface.[29,30] This may be mediated by their adsorption onto the hydrate surface, which effectively decreases the crystal

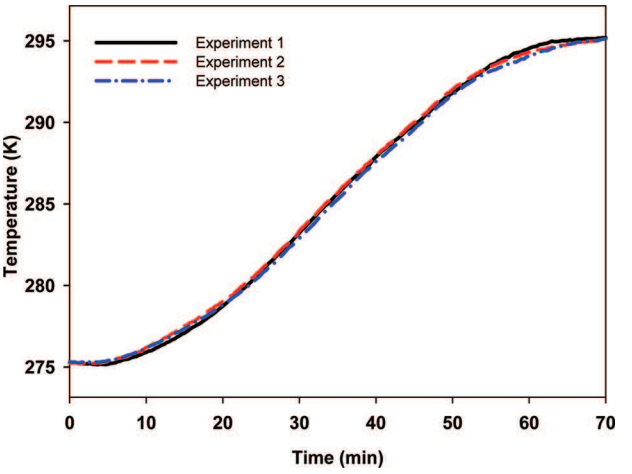

Figure 4. Temperature profiles for decomposition experiments (experiments 1, 2, and 3 from Table 1).

growth rate.[31−34] Gordienko et al.[35] similarly demonstrated that AFPs adsorb to THF hydrate, suggesting that both commercial and biological inhibitors likely inhibit hydrate growth by an adsorption−inhibition mechanism. Although Kvamme et al.[36] correlated hydrate−inhibitor interactions to binding strengths, it is not clear how these could differ because the molecules should either bind and be incorporated into the growing hydrate crystal at higher driving forces or over longer periods of time or not bind. Alternatively, we suggest that very effective KHIs, once close to the hydrate surface, have a high probability of being "anchored", using a chemical group that fills an empty cage, not only resulting in the inhibition of further crystal growth but also partially explaining the reduction in gas uptake. Such a model has been developed in silico for PVP on hydrates.[37] In such a model, H1W85281 would have the highest probability of incorporation into the hydrate crystal.

B. Hydrate Decomposition in the Presence of Inhibitors. Hydrates formed in the presence of inhibitors were decomposed by heating, which resulted in consistent melting profiles (Figure 4).

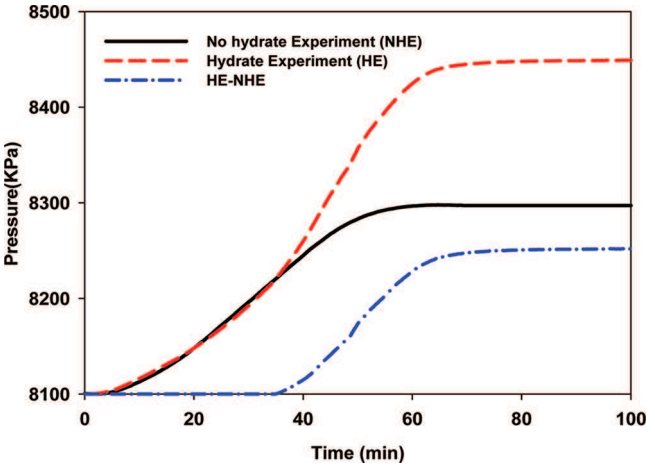

Figure 5. Pressure profiles for the no-hydrate experiment (NHE, gas expansion due to temperature increase), the hydrate experiment (HE, gas expansion due to temperature increase, and gas release due to decomposition of hydrate), and the difference (HE − NHE, gas release due to decomposition of hydrate).

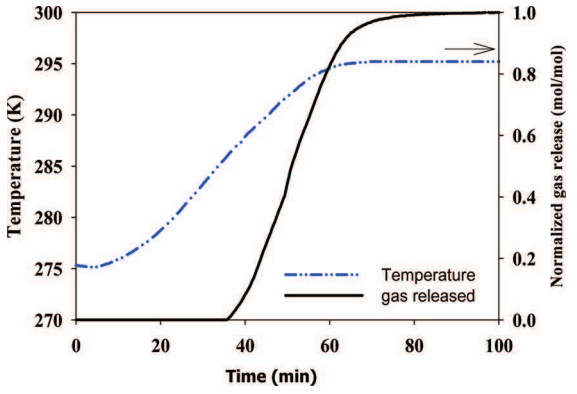

Figure 6. Typical gas hydrate decomposition, along with heating profile, for experiment 1 in Table 1.

The heating profiles for the other experiments are not shown.[38] The increase in the pressure generated by decomposition was also consistent, as demonstrated by Figure 5, which shows the pressure profile of two experiments conducted under the same experimental conditions. In the absence of formed hydrate, increased pressure was solely due to gas expansion as temperature increased, with a much higher pressure associated with decomposition of hydrates. A typical decomposition curve obtained after accounting for the gas expansion is shown in Figure 6. The normalized hydrate decomposition profiles for all the systems investigated are shown in Figure 7. It is clearly evident from the figure that decomposition started later in the absence of inhibitors and was consistent between experiments (Figure 8). The complete decomposition of the hydrates formed in the presence of the commercial KHIs, PVP and HIW85281, appeared to be in two stages and was so protracted that maximum pressures were not achieved until after the control samples (water only) had decomposed (Figure 8b and c). These observations are not surprising, as it has been previously reported that kinetic inhibitors can increase the temperature[39,40] or the time[19,41] required for complete hydrate decomposition.

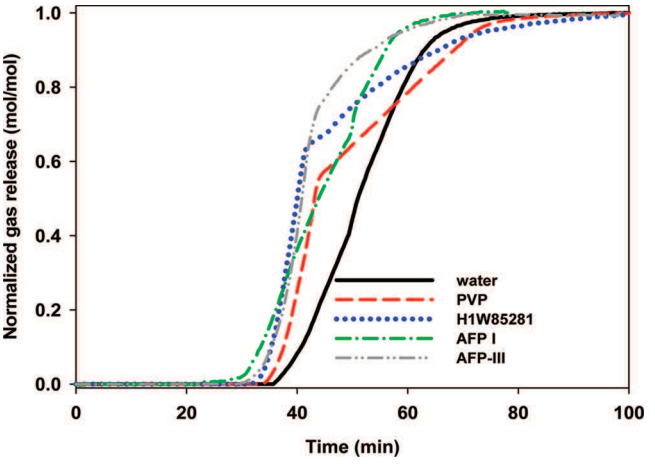

Figure 7. Normalized gas release profiles in the presence of inhibitors (experiments 1, 7, 9, 13, and 17).

A two-stage hydrate decomposition profile may be due to inhomogeneous hydrate formation, composed of both structure I and II hydrate, as has been previously reported in mixed gases of methane and ethane as well as in more complex natural gas mixtures.[15,16,42,43] Makogon and Holditch[39,40] reported that the presence of KHIs increased the temperature at which hydrates completely decomposed. It is noteworthy, too, that Schicks et al.[43] reported that the hydrate decomposition line shifted toward higher temperatures with increasing concentrations of ethane and propane in a gas mixture. Thus, it is possible that heavier hydrocarbons participate to a greater extent in hydrate formation, which likely has a heterogeneous crystal structure, in the presence of the commercial KHIs. In an alternative but related explanation, a new hydrate, possibly of a different composition, could form subsequent to the temperature drop induced by the ongoing dissociation of the existing hydrate and/or the changing gas mixture composition. This newly formed hydrate may even act as an impurity in hydrates of a different composition. Also, because melting temperatures can vary depending on the hydrate dimension (<1 μm), commercial KHIs could also have an impact on crystal size.

In contrast to the two-stage decomposition observed with the commercial KHIs, the hydrate melting profiles with the two biological inhibitors were strikingly simpler. Single-stage decompositions, more similar to the water controls, albeit at lower temperatures, were seen in the presence of AFP-I and AFP-III (Figure 8d and e). As well, unlike the case with PVP or H1W85281, there was such a rapid decomposition that the overall melting period was even less than that required for hydrates formed in the absence of any inhibitors (Figure 7). These observations are consistent with our previous study on hydrate formation and decomposition using high pressure differential scanning calorimetry (HP-DSC), in that multiple endothermic peaks were observed with the commercial KHIs in contrast to the less complex profiles seen with AFP-III.[27] Although the reasons for this distinct behavior in the two types of inhibitors are unknown, we speculate that crystals formed in the AFP-containing solutions were more homogeneous, consistent with a sharp melting profile, and that the incorporation of the protein resulted in less stable crystals, which decomposed at lower temperatures compared to those formed in the presence of the commercial KHIs. For a better understanding of these

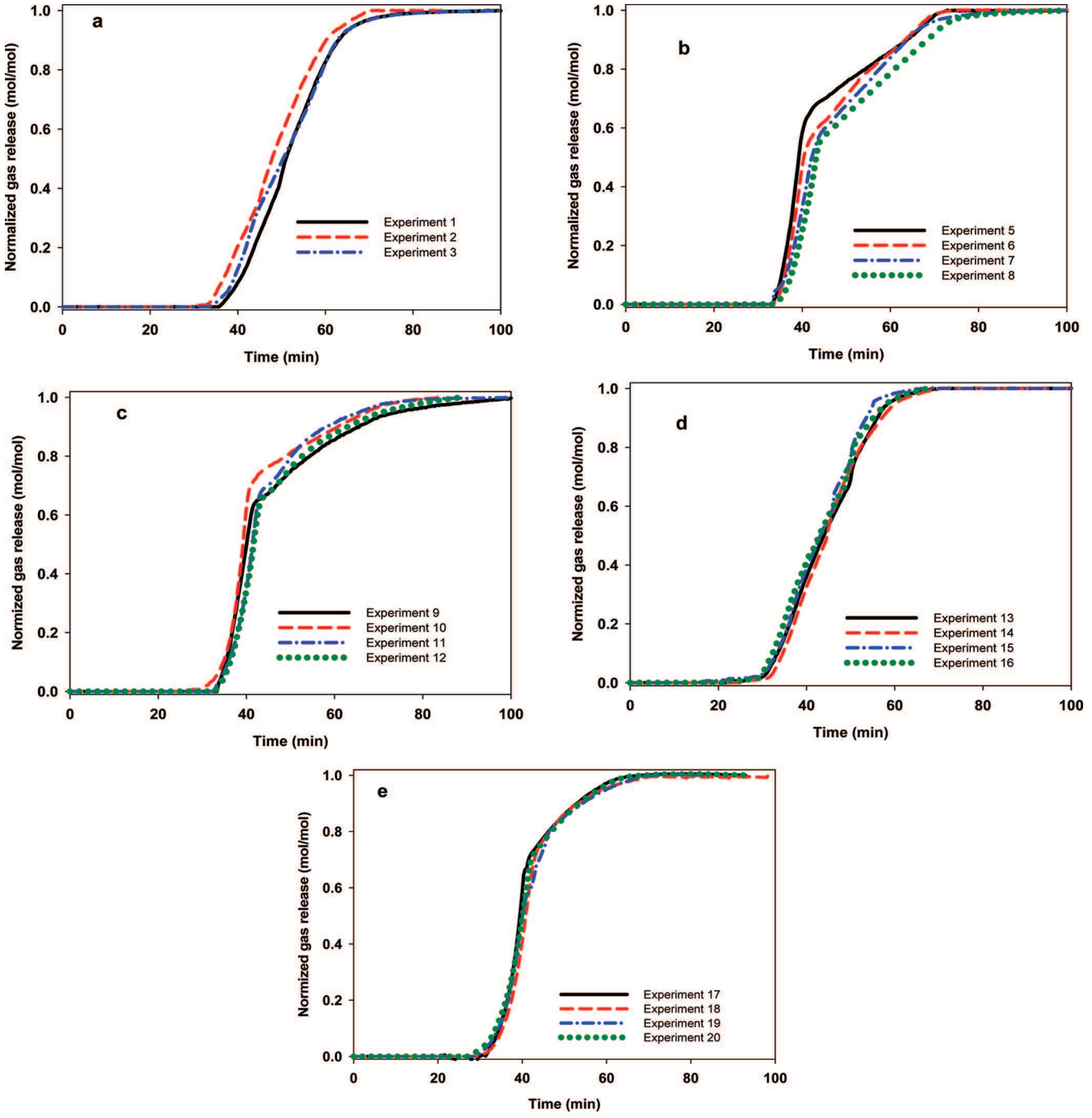

Figure 8. Normalized gas release profiles in the presence of (a) water, (b) PVP, (c) H1W85281, (d) AFP-I, and (e) AFP-III.

complex observations, the compositional and structural analyses using GC, XRD, and Raman and NMR spectroscopy are presented as Part 3 of this series.[44]

IV. CONCLUSIONS

A newly fabricated stirred reactor operated at a constant pressure and temperature allowed a direct comparison of the formation and dissociation of mixed gas hydrates in the presence of commercial and biologically based kinetic hydrate inhibitors (KHIs). All inhibitors significantly delayed hydrate nucleation and reduced the hydrate growth. The new commercial inhibitor H1W85281 was the most effective in prolonging the induction time (by a factor of 33.6) and reducing growth (by a factor of 2.2) compared to the other tested inhibitors. These analyses confirm that KHIs perform both as nucleation inhibitors and growth inhibitors, and such properties may reflect different mechanisms of action. A two-stage decomposition of hydrates formed in the presence of the two commercial inhibitors is suggestive of heterogeneous hydrate crystals, consistent with our previous study using calorimetry as well as the observations of other researchers. In contrast, hydrates formed in the presence of either AFP type decomposed in a manner similar to that observed for

no KHI controls but faster. Although the probability of hydrate formation can be reduced with KHIs, unusual circumstances, such as long shut-in periods, can nevertheless result in hydrate formation and plugging of pipelines. In these cases, decomposition kinetics in the presence of inhibitors is an important factor for consideration. Use of biological inhibitors not only delays nucleation and inhibits hydrate growth, but when conditions change, hydrates formed in the presence of AFPs show complete decomposition at an earlier time, an advantageous and valuable attribute for any KHI.

AUTHOR INFORMATION

Corresponding Author

*Phone: +1 604-822-6184. Fax: +1604-822-6003. E-mail: englezos@interchange.ubc.ca.

ACKNOWLEDGMENT

We thank Shell Global Solutions for their suggestions and encouragement. The financial support from the Natural Sciences and Engineering Research Council of Canada (NSERC) is greatly appreciated.

REFERENCES

(1) Sloan, E. D.; Koh, C. A. *Clathrate Hydrates of Natural Gases*, 3rd ed.; CRC Press, Taylor & Francis Group: New York, 2008.

(2) Sloan, E. D. *Clathrate Hydrates of Natural Gases*; Marcel-Dekker, Inc.: New York, 1998; p 664.

(3) Freer, E.; Sloan, E. D. An engineering approach to kinetic inhibitor design using molecular dynamics simulations. *Ann. N. Y. Acad. Sci.* **2000**, *912*, 651.

(4) Kelland, M. A. History of the development of low dosage hydrate inhibitors. *Energy Fuels* **2006**, *20* (3), 825–847.

(5) Walker, V. K.; Zeng, H.; Gordienko, R.; Kuiper, M. J.; Huva, E. I.; Ripmeester, J. A. The mysteries of memory effect and its elimination with antifreeze proteins. *Proceedings of 6th International Conference on Gas Hydrates*, Vancouver, July 2008.

(6) Zeng, H.; Moudrakovski, I. L.; Ripmeester, J. A.; Walker, V. K. Effect of antifreeze protein on nucleation, growth and memory of gas hydrates. *AIChE J.* **2006**, *52* (9), 3304–3309.

(7) Zeng, H.; Wilson, L. D.; Walker, V. K.; Ripmeester, J. A. The inhibition of tetrahydrofuran clathrate−hydrate formation with antifreeze protein. *Can. J. Phys.* **2003**, *81* (1−2), 17–24.

(8) Zeng, H.; Wilson, L. D.; Walker, V. K.; Ripmeester, J. A. Effect of antifreeze proteins on the nucleaton, growth, and the memory effect during tetrahydrofuran clathrate hydrate formation. *J. Am. Chem. Soc.* **2006**, *128* (9), 2844–2850.

(9) Al-Adel, S.; Dick, J. A. G.; El-Ghafari, R.; Servio, P. The effect of biological and polymeric inhibitors on methane gas hydrate growth kinetics. *Fluid Phase Equilib.* **2008**, *267* (1), 92–98.

(10) Ohno, H.; Susilo, R.; Gordienko, R.; Ripmeester, J.; Walker, V. K. Interaction of antifreeze proteins with hydrocarbon hydrates. *Chem.—Eur. J.* **2010**, *16* (34), 10409–10417.

(11) Yeh, Y.; Feeney, R. E. Antifreeze proteins: structures and mechanisms of function. *Chem. Rev.* **1996**, *96* (2), 601–617.

(12) Davies, P. L.; Baardsnes, J.; Kuiper, M. J.; Walker, V. K. Structure and function of antifreeze proteins. *Philos. Trans. R. Soc. London* **2002**, *357* (1423), 927–933.

(13) Jensen, L.; Thomsen, K.; von Solms, N. Inhibition of structure I and II gas hydrates using synthetic and biological kinetic inhibitors. *Energy Fuels* **2011**, *25*, 17–23.

(14) Seo, Y.; Kang, S. P.; Jang, W. Structure and composition analysis of natural gas hydrates: C-13 NMR spectroscopic and gas uptake measurements of mixed gas hydrates. *J. Phys. Chem. A* **2009**, *113* (35), 9641–9649.

(15) Uchida, T.; Takeya, S.; Kamata, Y.; Ohmura, R.; Narita, H. Spectroscopic measurements on binary, ternary, and quaternary mixed-gas molecules in clathrate structures. *Ind. Eng. Chem. Res.* **2007**, *46* (14), 5080–5087.

(16) Kumar, R.; Linga, P.; Moudrakovski, I.; Ripmeester, J. A.; Englezos, P. Structure and kinetics of gas hydrates from methane/ethane/propane mixtures relevant to the design of natural gas hydrate storage and transport facilities. *AIChE J.* **2008**, *54* (8), 2132–2144.

(17) Rydzy, M. B.; Schicks, J. M.; Naumann, R.; Erzinger, J. Dissociation enthalpies of synthesized multicomponent gas hydrates with respect to the guest composition and cage occupancy. *J. Phys. Chem. B* **2007**, *111* (32), 9539–9545.

(18) Nihous, G. C.; Kuroda, K.; Lobos-Gonzalez, J. R.; Kurasaki, R. J.; Masutani, S. M. An analysis of gas hydrate dissociation in the presence of thermodynamic inhibitors. *Chem. Eng. Sci.* **2010**, *65* (5), 1748–1761.

(19) Bruusgaard, H.; Lessard, L. D.; Servio, P. Morphology Study of Structure I Methane Hydrate Formation and Decomposition of Water Droplets in the Presence of Biological and Polymeric Kinetic Inhibitors. *Cryst. Growth Des.* **2009**, *9* (7), 3014–3023.

(20) Nakagawa, R.; Akihiro, H.; Shoji, H. Dissociation and specific heats of gas hydrates under submarine and sublacustrine environments. *Proceedings of 6th International Conference on Gas Hydrates*, Vancouver, July 2008.

(21) Vysniauskas, A.; Bishnoi, P. R. A Kinetic-Study of Methane Hydrate Formation. *Chem. Eng. Sci.* **1983**, *38* (7), 1061–1072.

(22) Englezos, P.; Kalogerakis, N.; Dholabhai, P. D.; Bishnoi, P. R. Kinetics of formation of methane and ethane gas hydrates. *Chem. Eng. Sci.* **1987**, *42* (11), 2647–2658.

(23) Englezos, P.; Kalogerakis, N.; Dholabhai, P. D.; Bishnoi, P. R. Kinetics of gas hydrate formation from mixtures of methane and ethane. *Chem. Eng. Sci.* **1987**, *42* (11), 2659–2666.

(24) Cohen, J. M.; Wolf, P. F.; Young, W. D. Enhanced hydrate inhibitors: powerful synergism with glycol ethers. *Energy Fuels* **1998**, *12* (2), 216–218.

(25) McCallum, S. D.; Riestenberg, D. E.; Zatsepina, O. Y.; Phelps, T. J. Effect of pressure vessel size on the formation of gas hydrates. *J. Pet. Sci. Eng.* **2007**, *56* (1−3), 54–64.

(26) Linga, P.; Kumar, R.; Englezos, P. Gas hydrate formation from hydrogen/carbon dioxide and nitrogen/carbon dioxide gas mixtures. *Chem. Eng. Sci.* **2007**, *62* (16), 4268–4276.

(27) Daraboina, N.; Ripmeester, J. A.; Walker, V. K.; Englezos, P. Natural gas hydrate formation and decomposition in the presence of kinetic inhibitors. 1. High pressure calorimetry. *Energy Fuels* **2011**, DOI: 10:10.21/ef200812m.

(28) Englezos, P. Nucleation and Growth of Gas Hydrate Crystals in Relation to "Kinetic Inhibition. *Rev. IFP* **1996**, *51* (6), 789.

(29) Moon, C.; Taylor, P. C.; Rodger, P. M. Computer modelling of gas hydrate formation. *Proceedings of the 4th International Conference on Gas Hydrates*, Yokohama, Japan, May 19−23, 2002; pp 665−668.

(30) Moon, C.; Taylor, P. C.; Rodger, P. M. Molecular dynamics study of gas hydrate formation. *J. Am. Chem. Soc.* **2003**, *125* (16), 4706–4707.

(31) Kumar, R.; Lee, J. D.; Song, M.; Englezos, P. Kinetic inhibitor effects on methane/propane clathrate hydrate-crystal growth at the gas/water and water/*n*-heptane interfaces. *J. Cryst. Growth* **2008**, *310* (6), 1154–1166.

(32) Carstensen, A.; Creek, J. L.; Koh, C. A. Investigating the performance of clathrate hydrate inhibitors using in situ Raman spectroscopy and differential scanning calorimetry. *Am. Mineral.* **2004**, *89* (8−9), 1215–1220.

(33) King, H. E., Jr.; Hutter, J. L.; Lin, M. Y.; Sun, T. Polymer conformations of gas-hydrate kinetic inhibitors: a small-angle neutron scattering study. *J. Chem. Phys.* **2000**, *112* (5), 2523–2532.

(34) Anderson, B. J.; Tester, J. W.; Borghi, G. P.; Trout, B. L. Properties of inhibitors of methane hydrate formation via molecular dynamics simulations. *J. Am. Chem. Soc.* **2005**, *127*, 17852–17862.

(35) Gordienko, R.; Ohno, H.; Singh, V. K.; Jia, Z. C.; Ripmeester, J. A.; Walker, V. K. Towards a green hydrate inhibitor: imaging antifreeze proteins on clathrates. *PLoS ONE* **2010**, *5* (2), e8953.

(36) Kvamme, B.; Kuznetsova, T.; Aasoldsen, K. Molecular dynamics simulations for selection of kinetic hydrate inhibitors. *J. Mol. Graphics Modell.* **2005**, *23* (6), 524–536.

(37) Wathen, B.; Kwan, P.; Jia, Z. C.; Walker, V. K.Modeling the interactions between poly(*n*-vinylpyrrolidone) and gas hydrates: factors involved in suppressing and accelerating hydrate growth. In *High Performance Computing Systems and Applications*; Kent, R. D., Sands, T. W., Eds.; Kluwer Academic Publishers: Norwell, MA, 2010; Vol. 5976, pp 117−133, 418.

(38) Daraboina, N. Understanding the action of gas hydrate kinetic inhibitors. *Ph.D Dossier, University of British Columbia*, 2011.

(39) Makogon, Y. F.; Holditch, S. A. Gas hydrates—conclusion: experiments illustrate hydrate: morphology, kinetics. *Oil Gas J.* **2001**, *99* (7), 45–50.

(40) Makogon, Y. F.; Holditch, S. A. Lab work clarifies gas hydrate formation, dissociation. *Oil Gas J.* **2001**, *99* (6), 47–48. 50–52.

(41) Lee, J. D.; Englezos, P. Unusual kinetic inhibitor effects on gas hydrate formation. *Chem. Eng. Sci.* **2006**, *61* (5), 1368–1376.

(42) Subramanian, S. Measurements of clathrate hydrates containing methane and ethane using Raman spectroscopy. Ph.D. Thesis, Colorado School of Mines, Golden, CO, 2000.

(43) Schicks, J. M.; Naumann, R.; Erzinger, J.; Hester, K. C.; Koh, C. A.; Sloan, E. D. Phase transitions in mixed gas hydrates: experimental observations versus calculated data. *J. Phys. Chem. B* **2006**, *110* (23), 11468–11474.

(44) Daraboina, N.; Ripmeester, J. A.; Walker, V. K.; Englezos, P. Natural gas hydrate formation and decomposition in the presence of kinetic inhibitors. 3. Structural and compositional changes. *Energy Fuels* **2011**, DOI: 10.1021/ef200814z.